An optimized protocol for hip joint centre determination using the functional method

Valentina Camomilla*, Andrea Cereatti, Giuseppe Vannozzi, Aurelio Cappozzo

Department of Human Movement and Sport Sciences, Istituto Universitario di Scienze Motorie, Piazza Lauro de Bosis, 15, 00194 Roma, Italy

Abstract

The functional method identifies the hip joint centre (HJC) as the centre of rotation of the femur relative to the pelvis during an ad hoc movement normally recorded using stereophotogrammetry. This method may be used for the direct determination of subject-specific HJC coordinates or for creating a database from which regression equations may be derived that allow for the prediction of those coordinates. In order to contribute to the optimization of the functional method, the effects of the following factors were investigated: the algorithm used to estimate the HJC coordinates from marker coordinates, the type and amplitude of the movement of the femur relative to the pelvis, marker cluster location and dimensions, and the number of data samples. This was done using a simulation approach which, in turn, was validated using experiments made on a physical analogue of the pelvis and femur system. The algorithms used in the present context were classified and, in some instances, modified in order to optimize both accuracy and computation time, and submitted to a comparative evaluation. The type of movement that allowed for the most accurate results consisted of several flexion-extension/abduction-adduction movements performed on vertical planes of different orientations, followed by a circumduction movement. The accuracy of the HJC estimate improved, with an increasing rate, as a function of the amplitude of these movements. A sharp improvement was found as the number of the photogrammetric data samples used to describe the movement increased up to 500. For optimal performance with the recommended algorithms, markers were best located as far as possible from each other and with their centroid as close as possible to the HJC. By optimizing the analytical and experimental protocol, HJC location error not caused by soft tissue artefacts may be reduced by a factor of ten with a maximal expected value for such error of approximately 1 mm.
© 2005 Elsevier Ltd. All rights reserved.

Keywords: Movement analysis; Stereophotogrammetry; Biomechanics; Joint kinematics; Functional method; Centre of rotation; Hip joint

1. Introduction

Following the generally accepted hypothesis that a normal hip joint may be modelled as a spherical joint, the centre of rotation (CR) of the femur relative to the pelvis coincides with the geometrical centre of the acetabulum and, within a normal range of motion, of the femoral head. This point is referred to as hip joint centre (HJC). In human movement analysis the HJC is used to define the anatomical frame of the femur (Cappozzo et al., 1995; Wu et al., 2002) and as the reduction point of the external loads when estimating the hip muscular moment. As such, it affects both hip and knee joint kinematics and kinetics descriptions (Stagni et al., 2000). For this reason, the accuracy with which the 3-D HJC location is determined is of paramount importance and considered by human movement analysts to be a critical challenge for the future (Alderink et al., 2000; Holden and Stanhope, 1998; Kirkwood et al., 1999; Piazza et al., 2001; Besier et al., 2003; Piazza et al., 2004).

*Corresponding author. Tel.: +39 06 36733518;
fax: +39 06 36733517.
E-mail addresses: cappozzo@iusm.it, camomilla@iusm.it
(V. Camomilla).

In the majority of the investigations carried out through the late 1980s, the subject-specific location of the HJC was based on the 2-D or 3-D trajectories of markers located on the greater trochanter. It has subsequently been shown that this approach led to errors that were unacceptable in most applications (Cappozzo, 1991; Neptune and Hull, 1995). The most straightforward alternative method is 3-D medical imaging (roentgen-photogrammetry or tomography). However, this method is normally not available to movement analysis laboratories and may be regarded as invasive. In addition, its precision and accuracy are still to be evaluated in this context. Two other methods are most often used: the predictive and the functional methods.

The predictive method uses regression equations that provide an estimate of the coordinates of the HJC in a pelvic anatomical frame (PAF, Fig. 1) as a function of anthropometric quantities. Regression parameters have been obtained by analysing relatively small samples of isolated pelvises (Seidel et al., 1995) or, in vivo, through medical imaging (Andriacchi et al, 1980; Bell et al., 1989, 1990; Crowninshield et al., 1978; Davis et al., 1991; Tylkowski et al., 1982). No separate analyses have been performed on homogeneous samples of subjects in terms of gender, age (Fieser et al., 2000; Jenkins et al., 2000), race or anthropomorphic traits. The mean error with which the position of the HJC may be predicted in able-bodied adult male subjects using the available regression equations was estimated in the range of 25–30 mm (Bell et al., 1990; Leardini et al., 1999). Thus, more accurate and population-specific regression equations are required.

The functional method identifies the HJC as the relevant CR. To this purpose, an ad hoc experiment is carried out in the stereophotogrammetric laboratory. Subjects are asked to move their femur relative to their pelvis, and the global trajectories of markers located on both 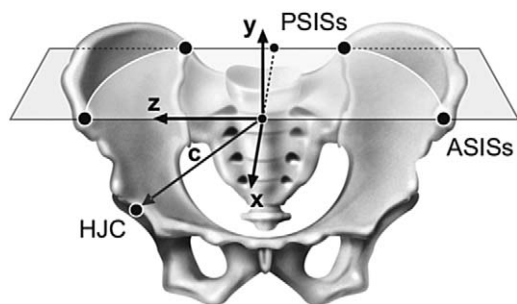pelvis (pelvic marker cluster) and thigh (femoral marker cluster) are reconstructed. The instantaneous positions of the femoral markers are represented in the PAF (Fig. 1) and fed to an algorithm which estimates the CR coordinates in the latter frame. According to an investigation carried out by Bell et al. (1990) using six subjects, this method allows for errors in the range of 16–65 mm, while Leardini et al. (1999), using eleven subjects, found errors in the range of 8–16 mm. It is reasonable to hypothesise that the latter accuracy can be generally attained or even improved upon, provided that good practice guidelines are determined and applied (Leardini et al., 1999; Piazza et al., 2001, 2004). Thus, this method may effectively be used for subject-specific HJC determination, except when patients with reduced hip mobility are dealt with. In addition, this method may allow for the collection of large amount of data from which predictive models, more reliable than presently available, can be derived (Lenhoff et al., 1998).

Because of the above-illustrated relevance of the functional approach for HJC determination, the optimization of the analytical and experimental procedures involved is indeed worthwhile pursuing (Piazza et al., 2004). The objective of the present paper is to contribute to the completion of this optimization. In particular, it deals with the refinement and comparative evaluation of the algorithms used to estimate the CR under different experimental conditions. The experimental conditions were described by using quantities that are known to affect both precision and accuracy of the estimates (henceforth referred to as inaccuracy factors):

1. stereophotogrammetric error,
2. type and amplitude of the relative movement between pelvis and femur,
3. marker position data density (related to frame rate and movement speed),
4. geometry and location of the femoral marker cluster.

Two approaches were used. First, a mathematical simulation tested the algorithms under several possible experimental conditions. Second, a set of experiments, carried out in the stereophotogrammetric laboratory on a mechanical linkage simulating the hip joint, aimed at validating the simulation results.

Soft tissue artefacts and the misidentification of pelvic anatomical landmarks have virtually no interaction with the inaccuracy factors listed above and their investigation calls for different methodological approaches; thus, they will be dealt with in a separate study.

Fig. 1. Pelvic anatomical frame defined as follows: the origin is the midpoint between the anterior superior iliac spines (ASISs); the z-axis is defined as the line passing through the ASISs with its positive direction from left to right; the x-axis lies in the quasi transverse plane defined by the ASISs and the midpoint between the posterior superior iliac spines (PSISs) with its positive direction forwards; the y-axis is orthogonal to the xz plane with its positive direction proximal. Vector **c** identifies the HJC position with respect to this reference frame.

2. Review of the algorithms

All analytical methods proposed in the literature for estimating the CR using reconstructed marker positions make the basic assumption that the distance between

femoral markers, or their centroid, and the CR does not vary.

One category of analytical methods entails no geometric constraints between markers and imposes that each femoral marker, or the centroid, lies on a spherical surface, the centre of which is the CR, during movement. These methods have been implemented using three analytical approaches: one is based on a quadratic best sphere fitting procedure (S2 method) (Cappozzo, 1984; Silaghi et al., 1998); the second uses a quartic best sphere fitting procedure (S4 method) (Gamage and Lasenby, 2002); the third is based on the Reuleaux method (RE method) and determines the CR as the quasi-intersection between mid-orthogonal planes to vectors connecting each marker position in two arbitrarily chosen instants of time (Halvorsen et al., 1999).

Another category of methods imposes that the distance between femoral markers must be invariant, i.e. the femoral marker cluster must be rigid. The CR is determined as the point of this rigid body endowed with minimal displacements relative to the PAF, in a least squares sense (MD method; Holzreiter, 1991). The CR may also be determined as the closest point (pivot point), in a least squares sense, to the ensemble of finite helical axes, each corresponding to two selected poses of the above-mentioned rigid body (FA method) (Woltring, 1990).

Several authors have attempted to rationalize this subject matter. Algorithms that were supposed to be different were shown to be, under specified conditions, analytically identical. This was the case for the methods RE and S4 as proposed by Halvorsen et al. (1999) and Gamage and Lasenby (2002), respectively. These were found to coincide when in the RE method all possible combinations of marker positions and, thus, of displacements, were exploited (Halvorsen, 2002; Cereatti et al., 2004). Moreover, Halvorsen (2002) has demonstrated that the MD and FA methods coincide when, for both methods, all possible combinations of marker cluster poses are used and, for the FA method, the contribution of the individual helical axes is weighted by a function of the relevant rotation angle.

Halvorsen (2002) showed that the S4, MD, and FA methods led to biased solutions caused by photogrammetric errors. A bias compensation procedure was, thereafter, proposed for the S4 method that was effective under the hypothesis that the errors were isotropic, zero-mean and normally distributed (Halvorsen, 2002, 2003).

3. Materials and methods

3.1. Selected algorithms for the hip joint centre estimation

The HJC position vector in the PAF was referred to as **c** and its true (nominal) and estimated values as $\mathbf{c}_n$
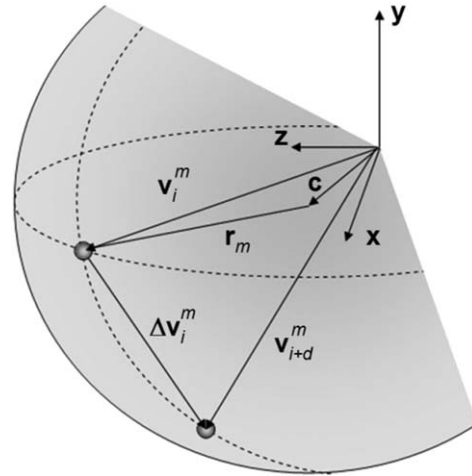

Fig. 2. The set of axes *x, y, z* is rigid with respect to the pelvic reference frame, PAF. $\mathbf{v}_i^m$ is the position vector of the *m*th marker associated with the femur in the *i*th sampled instant of time. $\mathbf{v}_{i+d}^m$ is relative to the *(i+d)*th sampled instant of time and $\Delta\mathbf{v}_i^m = \mathbf{v}_i^m - \mathbf{v}_{i+d}^m$ is the displacement of the *m*th marker. CR is the centre of rotation of the femoral segment relative to the pelvis; **c** is its position vector in the PAF. $\mathbf{r}^m$ is the radius of the sphere defined by the *m*th marker.

and **ĉ**, respectively. The determination of **ĉ** was based on the position vectors of *M* femoral markers in the PAF ($\mathbf{v}_i^m$; $i = 1, \ldots, N$; $m = 1, \ldots, M$) in *N* sampled instants of time (Fig. 2). Clusters consisting of more than four markers were not used because, in the presence of stereophotogrammetric error only, they would not have allowed for a significantly better pose estimate (Cappozzo et al., 1997).

3.1.1. Centre of the quadratic best fitted sphere (S2)

The CR was determined minimizing the quadratic objective function in the form proposed by Cappozzo (1984):

$$f(\mathbf{c}, r) = \sum_{i=1}^{N} (||\bar{\mathbf{v}}_i - \mathbf{c}|| - r)^2, \tag{1}$$

where $\bar{\mathbf{v}}_i = (1/M)\sum_{m=1}^{M} \mathbf{v}_i^m$ is the marker centroid position vector, and *r* is the radius of the sphere defined by the latter point. Minimization of this function required a first approximation value for **c** (determined, for example, using a predictive method) and was accomplished through an iterative procedure based on the simplex method (Lagarias et al., 1998).

The S2 method has already been described as having a modest performance (Gamage and Lasenby, 2002). However, a thorough comparative assessment has not been reported and many biomechanists still use it (Hicks et al., 2003; Aguinaldo et al., 2003; Schwartz and Rozumalski, 2003).

3.1.2. Centre of the bias-compensated quartic best fitted sphere (S4)

The CR was determined through a closed form minimization of the quartic objective function (Gamage and Lasenby, 2002):

$$f(\mathbf{c}, r^m) = \sum_{m=1}^{M} \sum_{i=1}^{N} \left[||\mathbf{v}_i^m - \mathbf{c}||^2 - (r^m)^2\right]^2, \tag{2}$$

where r^m is the radius of the sphere defined by the mth marker. The bias that affects the solution of Eq. (2) is compensated for by solving it iteratively using, at each iteration, the previous solution as initial estimate and introducing a correction term, which incorporates the latter estimate and a model of the photogrammetric error, detailed in Halvorsen (2003).

3.1.3. Minimal linear displacement point (MD)

The femoral marker cluster is assumed to be rigid. Let d be a number of sampled instants of time. Then the cluster's movement in the PAF, from the ith position to the $(i+d)$th position, can be characterized by a translation vector ${}^{i+d}\mathbf{t}_i$ and an orientation matrix ${}^{i+d}\mathbf{R}_i$, $(i = 1, \ldots, N)$.

The position vector of the femoral marker cluster centroid after movement is given by

$$\bar{\mathbf{v}}_{i+d} = {}^{i+d}\mathbf{R}_i \bar{\mathbf{v}}_i + {}^{i+d}\mathbf{t}_i. \tag{3}$$

When shifting the system of reference by a vector $\mathbf{c}$, the initial translation vector ${}^{i+d}\mathbf{t}_i$ changes into a new translation vector ${}^{i+d}\mathbf{h}_i$.

$$\bar{\mathbf{v}}_{i+d} - \mathbf{c} = {}^{i+d}\mathbf{R}_i (\bar{\mathbf{v}}_i - \mathbf{c}) + {}^{i+d}\mathbf{h}_i \tag{4}$$

Supposing that the movement from one position to another occurs through a pure rotation about the CR, then ${}^{i+d}\mathbf{h}_i = 0$ (Holzreiter, 1991). Considering different movements, represented by a set of P transformation matrices, an average centre of rotation was found by minimizing the following least squares cost function:

$$f(\mathbf{c}) = \sum_{i=1}^{P} \left\|{}^{i+d}\mathbf{h}_i\right\|^2, \tag{5}$$

$$^{i+d}\mathbf{h}_i(\mathbf{c}) = (\bar{\mathbf{v}}_{i+d} - \mathbf{c}) - {}^{i+d}\mathbf{R}_i(\bar{\mathbf{v}}_i - \mathbf{c}). \tag{6}$$

The relevant orientation matrix, ${}^{i+d}\mathbf{R}_i$, was calculated as in Söderkvist and Wedin (1993). Minimization of the cost function was accomplished through its closed form solution, according to the Gauss–Markov theorem.

The selection of all possible transformation matrices leads to a set of $\frac{1}{2}N(N-1)$ transformations that entails $O(N^2)$ operations (Halvorsen, 2003). Taking into account potential computing time problems and the fact that transformation matrices associated with small movements are more sensitive to experimental errors, an alternative criterion was also used. The transformation matrices relative to the wider movements were selected using the following procedure: for $i = 1$, ${}^{i+d}\mathbf{R}_i$ was determined for d selected so that $\overline{\Delta \mathbf{v}_i} = \bar{\mathbf{v}}_{i+d} - \bar{\mathbf{v}}_i$ was maximum. Then the data set was rewritten so that it started from the former $(i+d)$th frame and the ith frame was removed. Using this new data set the procedure was reiterated until all data points were used. This criterion will be referred to as WM (widest movements) set. In this way, the method (MD–WM) guaranteed the exploration of all data samples and entailed $O(N)$ operations only.

3.1.4. Pivot point of weighted finite helical axes (FA)

The CR was determined as the point whose root mean square (rms) distance from the finite helical axes (FHAs), associated with selected finite movements of the femoral marker cluster, was minimal (Woltring, 1990). However, the estimation of the ith FHA, i.e. of the relevant position vector ($\mathbf{s}_i$) and versor ($\mathbf{n}_i$), is highly sensitive to measurement noise and its accuracy is inversely proportional to the rotation magnitude, θ_i (Woltring et al., 1985). This angle was thus used as a weighting term of the individual FHA parameters (w_i). Halvorsen (2002) used a weight related with the covariance matrices of $\mathbf{s}_i$ and $\mathbf{n}_i$, which, after Woltring et al. (1985), was set equal to $\sin(\theta_i/2)$.

The following objective function was minimized through the computation of its closed form solution:

$$f(\mathbf{c}) = \frac{2}{N(N-1)}$$
$$\times \sum_{i=1}^{N(N-1)/2} w_i \{(\mathbf{c} - \mathbf{s}_i) - [(\mathbf{c} - \mathbf{s}_i) \cdot \mathbf{n}_i]\mathbf{n}_i\}^2. \tag{7}$$

All possible combinations of marker cluster instantaneous poses were used (Halvorsen, 2002). This choice entails that $O(N^2)$ operations be carried out. Due to the simplicity of individual operations, computation time may be expected to be shorter than with the MD method, however larger than with the MD–WM method.

3.2. Simulation

Vectors $\mathbf{v}_i^m$ were generated to simulate all conditions of interest (inaccuracy factors). For this purpose, the following data were determined and used:

- realistic coordinates of the four pelvic anatomical landmarks and of the HJC ($\mathbf{c}_n$) in the PAF;
- the local coordinates of the femoral markers in an arbitrary femoral technical frame; four markers were located at the vertexes of a tetrahedron (side length, $l = 40$ to 240 step of 40 mm) and their centroid at a distance from the HJC ($\rho = 200$ to 1400 mm, step of 200 mm; the maximal value simulated markers located on a shank supposed to be rigid with the thigh);

Table 1
Description of the lower limb movements relative to the pelvis

Movement		Description
Cross		Flexion of 30°, neutral position, extension of 30°, neutral position, abduction of 30°, neutral position.
Arc		Flexion of 30°, half circumduction to extension of 30°, neutral position.
Star		Seven flexion-extension/abduction-adduction combined movements from the neutral position within the perimeter drawn in the *Arc* movement.
StarArc		*Star* movement followed by *Arc* movement

Plots indicate the trajectory of the foot as seen from above. Angles are defined according to the convention described in Grood and Suntay, 1983. The internal–external rotation angle was given a null value.

- a gaussian, zero-mean noise (standard deviation: $e_s = 1.0$ mm) that simulated the photogrammetric error (Della Croce and Cappozzo, 2000);
- hip motion types defined as in Table 1;
- nominal range of motion of the hip in the sagittal and frontal planes equal to 60° and 30°, respectively (flexion-extension, abduction-adduction); these values were chosen as conservative limits (50% of the maximum) of the hip range of motion, with the knee extended, normally attainable by a young adult (Kapandji, 1987);
- range of motion divider ($div = 0.5, 1, 2, 4$) aimed at simulating different hip movement amplitudes;
- number of data points within the movement observation interval of time ($N = 100$ to 1500).

Uniformly spaced samples of the orientation matrix and position vector of the femoral technical frame relative to the PAF were generated for each movement type and amplitude. Given the local coordinates of the four femoral markers, their nominal trajectories in the PAF were calculated. These coordinates and those of the pelvic markers were corrupted with simulated noise realizations (e_s). The corrupted femoral marker coordinates were thereafter recalculated in the corrupted PAF. This procedure aimed at reproducing realistic experimental conditions. The estimate of the CR, $\hat{\mathbf{c}}$, was then determined in the PAF using the algorithms described above. For each set of inaccuracy parameter values, that is for each trial, the determination of $\hat{\mathbf{c}}$ and of the relevant error $\mathbf{e} = \mathbf{c}_n - \hat{\mathbf{c}}$, was iterated fifty times, using different noise series. Biases (b_x, b_y, b_z, b_a) and standard deviations ($\sigma_x, \sigma_y, \sigma_z, \sigma_a$) of vector $\mathbf{e}$ components (e_x, e_y, e_z) and amplitude (e_a) were estimated over these fifty values. Maximal expected errors ($\delta_x, \delta_y, \delta_z, \delta_a$),

associated with a given set of parameters and a given method, were estimated as the sum of the relevant bias plus twice the standard deviation.

3.3. The mechanical linkage

A mechanical device, consisting of two rigid segments connected by a ball and socket joint, was built based on the dimensions of the human pelvis and femur. Four markers were located in fixed positions on the pelvic element, and four markers were located at the vertexes of a tetrahedron ($l = 200$ mm) that could be moved along the femoral element (Fig. 3). The nominal position of the CR in the equivalent PAF was measured using a calliper with an error of less than 1 mm.

A nine-camera Vicon 612 motion analysis system (Oxford Metrics; UK) was used at 120 frames per second. The measurement volume was a 1.5 m sided cube. All movements in Table 1 were performed with two different ranges of motion ($div = 1, 2$) and two different marker cluster locations ($\rho = 300, 1000$ mm). The device was manually operated so that at least 500 samples were acquired. Three recordings were made for each configuration. Reconstructed marker trajectories were thereafter processed using the procedures described with reference to the simulated data.

4. Results

4.1. Algorithms

When using the S2 method, the inaccuracy of the first approximation value given to the vector $\mathbf{c}$ was found not to be critical. The different implementations of the MD
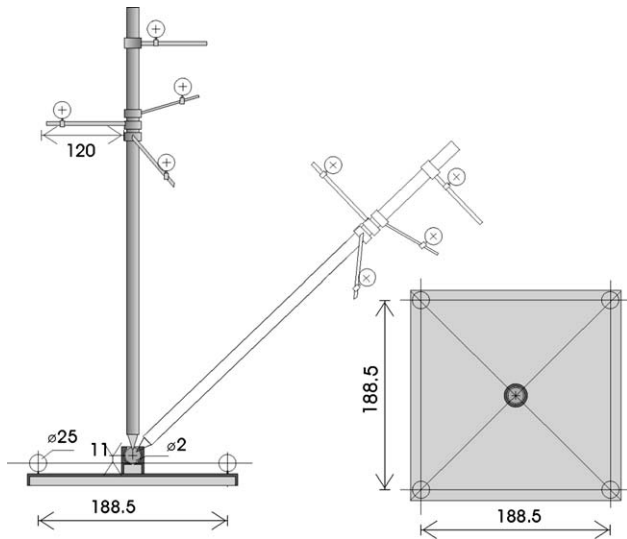
Fig. 3. Physical analogue of the femur-pelvis system. On every arm a marker was located. Cluster geometry could thus be modified by changing arm positions along the rod and marker position along the arms, allowing for the reproduction of different cluster dimensions (l) and cluster centroid distance from the CR (ρ). Measurements are in mm.

and FA algorithms were submitted to comparative analysis. In the MD method, the two criteria for the selection of the transformation matrices illustrated previously were shown to give similar results. When the WM criterion was used, the CR estimates were consistently less biased by approximately 10%. This result and the considerably lower computational time (for $N = 500$, $1{:}10^4$ ratio) proved that the latter implementation is preferable. In the FA method the comparative analysis showed that estimates were more accurate and precise when the weight θ_i was used in place of $\sin(\theta_i/2)$; δ_a, b_a, and σ_a, averaged over all the movements and ranges of motion analysed, were respectively 2.6, 10.7 and 1.3 times lower with the former than with the latter weight. Computation time of the MD–WM method, for $N = 500$, was a hundred times lower than that of the FA method and similar to that of the S4 method. In the subsequent analyses, the FA method with weight θ_i and the MD method, associated with the WM criterion, will be used.

4.2. Movements

The comparative evaluation of the errors associated with the various algorithms and for the selected movements and ranges of motion are reported for a specific marker cluster ($l = 200$ mm, $\rho = 300$ mm) and $N = 1000$ (Table 2). The reason why these values were chosen will be commented upon in the following sections.

The S2 method exhibited the overall worst maximal expected error for all movements analysed. The standard deviation σ_a ranged from 0.2 to 21.4 mm and the

bias b_a was relatively small (3–18 times smaller than σ_a). Both σ_a and b_a and their rate of variation increased as the hip movement amplitude decreased causing the maximal amplitude error δ_a to increase from 0.4 to 48.0 mm. For methods S4, MD, and FA, σ_a and b_a also increased as the hip movement range decreased, but both were always lower than 1.5 mm. The bias in the S4 method was lower than that yielded by the other methods. More detailed results are reported with respect to the latter three methods only.

The highest δ_a values were obtained with the *Cross* and with the *Star* movements, irrespective of the algorithm used, and were in the range 0.4–4.4 mm (Fig. 4). For the FA and MD methods, lower δ_a values were obtained with the *StarArc* than with the *Arc* movement and ranged from 0.3 mm ($div = 0.5$) to 2.6 mm ($div = 4$). The S4 method performed slightly better with the *Arc* movement: δ_a ranged from 0.3 mm ($div = 0.5$) to 2.1 mm ($div = 4$).

The maximal expected error was analysed along the different axes of the PAF. Irrespective of the method used, along the antero-posterior axis, δ_x was always lower than along the medio-lateral axis, δ_z, and the vertical, δ_y, axis. The average ratios δ_x/δ_y and δ_x/δ_z were 2:3. This result was expected since the X coordinate depends principally on the range of motion in the sagittal plane which is the largest, while the smaller range of motion in the frontal plane negatively affects both the Z and Y coordinates.

4.3. Number of data points

The effect of the number N was evaluated on the best performing movements. *StarArc* and *Arc*, for any given div value, yielded similar results. For $div = 1$ and all methods, for N increasing from 100 to 500 resulted in a reduction of δ_a from 2.2 mm to 0.8 mm (Fig. 5). Virtually no improvement was found for N greater than 500. The choice of $N = 1000$ for the present comparative analysis was conservative.

4.4. Marker cluster design

In the FA and MD methods, for any given cluster dimension, l, an increase of the cluster centroid distance from the CR, ρ, implied a linear increase of the error (Fig. 6a and b). Decreasing l caused the slope of the error curves to increase. For small clusters, $l = 40$ mm and ρ ranging from 200 to 1400 mm, the error for methods FA and MD changed from 3.5 to 24.2 mm, and from 2.2 to 15.8 mm, respectively. For large clusters, $l = 240$ mm and the same range of ρ the error changed from 0.4 to 1.6 mm and from 0.4 to 1.3 mm, respectively. For the S4 method, the error varied non-linearly from 0.5 to 1.4 mm along the entire range of l and ρ (Fig. 6c). The smallest ρ and largest l granted for the best results for all methods. The

Table 2
Standard deviation (σ_a) and bias (b_a) in millimetres, for all methods, movements, and range of motion dividers

Movement	Div	S2		S4		MD		FA	
		σ_a	b_a	σ_a	b_a	σ_a	b_a	σ_a	b_a
Cross	0.5	0.23	0.01	0.19	0.01	0.19	0.10	0.14	0.07
	1	0.79	0.05	0.36	0.03	0.34	0.17	0.28	0.17
	2	3.03	0.21	0.69	0.16	0.66	0.42	0.60	0.46
	4	21.39	5.19	1.38	0.68	1.31	1.19	1.37	1.47
Arc	0.5	0.24	0.05	0.14	0.03	0.17	0.20	0.10	0.09
	1	0.82	0.16	0.23	0.06	0.28	0.18	0.17	0.18
	2	3.16	0.70	0.45	0.10	0.52	0.14	0.35	0.38
	4	13.52	4.83	0.90	0.29	1.05	0.37	0.78	0.90
Star	0.5	0.27	0.07	0.21	0.05	0.18	0.03	0.20	0.06
	1	0.86	0.19	0.39	0.07	0.33	0.07	0.34	0.15
	2	3.12	0.61	0.74	0.19	0.65	0.25	0.69	0.41
	4	13.31	1.36	1.45	0.75	1.27	1.08	1.54	1.33
StarArc	0.5	0.20	0.03	0.13	0.02	0.14	0.01	0.12	0.04
	1	0.64	0.14	0.26	0.07	0.23	0.05	0.21	0.07
	2	2.31	0.71	0.49	0.19	0.44	0.19	0.44	0.15
	4	12.73	2.59	0.99	0.59	0.91	0.75	1.02	0.49

Cluster parameters were set to: $l = 200$ mm, $\rho = 300$ mm. Sample number was $N = 1000$.
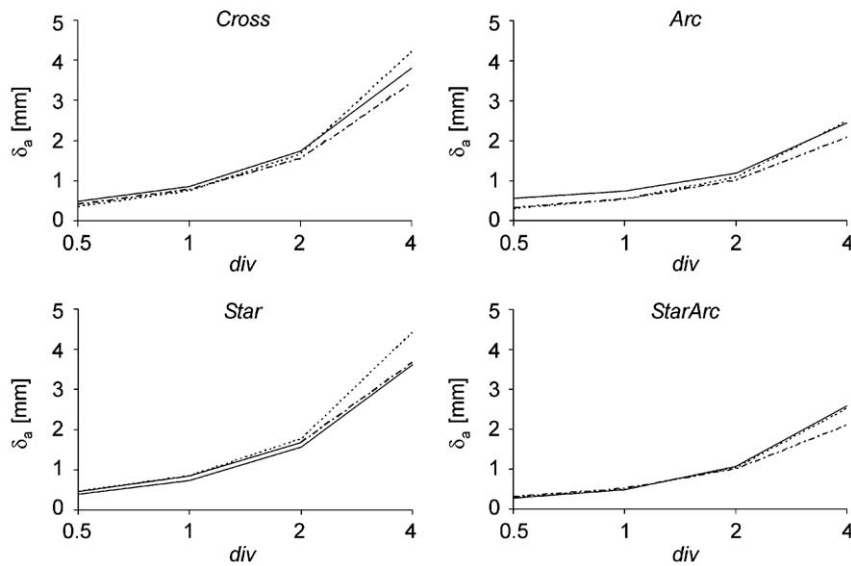

Fig. 4. Maximal expected error, δ_a, for all movements, range of motion dividers, and best performing algorithms (S4: dot-dashed line; MD: solid line; FA: dotted line).
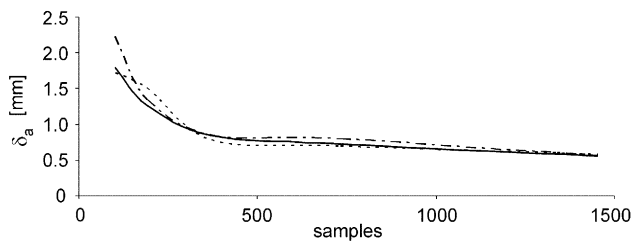

Fig. 5. Maximal expected error, δ_a, for methods S4 (dot-dashed line); MD (solid line), FA (dotted line), with the number of samples ranging from 100 to 1500. Data are relative to the *StarArc* movement.

S4 method exhibited a much lower sensitivity to cluster dimension than the other two methods. The marker cluster geometry and position ($\rho = 300$ mm and $l = 200$ mm) used for the above illustrated comparative analyses represented a choice of compromise consistent with experimental requirements.

4.5. Experimental validation

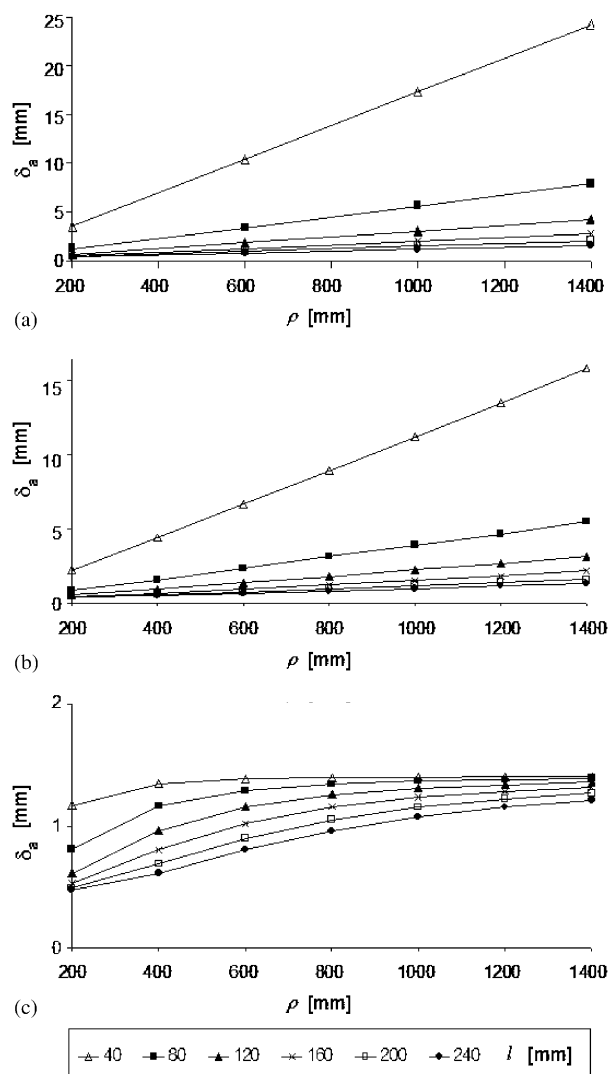The repeatability of the results yielded by the algorithms was estimated over 48 trials (3 repetitions × 4

Fig. 6. Maximal expected error, δ_a depicted as a function of ρ for methods FA (a), MD (b), and S4 (c). In each graph different curves correspond to different values of l, ranging from 40 to 240 mm, step 40 mm. Data are relative to the *StarArc* movement.

movement types $\times 2$ *div* $\times 2$ ρ). For S2, S4, MD, and FA, σ_a was found equal to 2.9, 1.3, 1.8, and 1.8 mm, respectively. Due to its poor repeatability, the S2 method was not included in the subsequent analyses. The standard deviations associated with different movements, obtained over 36 estimates (3 repetitions $\times 2$ *div* $\times 2\rho \times 3$ methods), were slightly higher for the *Cross* and for the *Star* movements, 1.8 mm, than for the *Arc* and *StarArc* movements, 1.6 and 1.2 mm, respectively. The reduction of the range of movement (from *div* = 1 to *div* = 2), analysed over 72 estimates (3 repetitions $\times 4$ movements $\times 2\rho \times 3$ methods), was found to increase σ_a from 1.4 to 1.6 mm. The change in cluster position ($\rho = 300$ and 1000 mm), analysed over 72 estimates (3 repetitions $\times 4$ movements $\times 2$ *div* $\times 3$ methods)

affected σ_a by raising it from 1.0 to 2.0 mm. These results were consistent with those obtained in the simulation exercise (Table 2, Fig. 6).

The determination of the accuracy with which the CR coordinates are estimated would entail knowing their nominal values with an error much lower than that associated with the estimate. This was not the case in the present analysis, in fact, the CR coordinates of the mechanical linkage could be measured with an error in the same range as that of the relevant estimates (1 mm). Accuracy was, therefore, evaluated in an alternative fashion by determining the number of estimates, obtained using selected parameters and methods, that fell within a range of ± 1 mm with respect to the nominal coordinate. Ninety-nine percent of the X, 48% of the Y and 92% of the Z coordinate estimates, out of 144 estimates (3 repetitions $\times 4$ movements $\times 2$ *div* $\times 2\rho \times 3$ methods), fell in the aforementioned range. These results indicate that the accuracy of the X and Z estimates was very close to that of direct measurement. Thus, only the results relative to the Y coordinate could be used for validating the simulation based comparative analysis. With reference to the best (*StarArc*) and worst (*Cross*) performing movements, these results were 67% and 28%, respectively, out of 36 estimates (3 repetitions $\times 2$ *div* $\times 2\rho \times 3$ methods). For ρ equal to 300 mm and 1000 mm, calculated over 72 estimates (3 repetitions $\times 4$ movements $\times 2$ *div* $\times 3$ methods), 80% and 17% were obtained, respectively. The reduction in the range of motion led to a change, calculated over 72 estimates (3 repetitions $\times 4$ movements $\times 2\rho \times 3$ methods), from 57% to 40%. These results are consistent with those obtained using simulation and confirm that the *StarArc* movement, the shortest distance of the cluster from the CR, and a wide range of motion allow for the most accurate coordinate estimates.

5. Discussion and conclusion

The precision and accuracy with which the HJC location is determined using the functional method has been shown to be sensitive to a number of analytical and experimental factors, and the data from this study can now be used to develop relevant good practice guidelines. However, the optimization process can be completed when soft movement artefacts and pelvic anatomical landmark identification errors are also taken into account in a future study.

Only one amplitude of the stereophotogrammetric error was simulated ($e_s = 1$ mm). Yet, all considerations drawn from the results thus obtained can be generalized taking advantage of the fact that, as Halvorsen (2002, 2003) has shown, the inaccuracy with which the HJC is estimated, in a double logarithmic scale, increases linearly for increasing values of e_s.

Different algorithms were selected, fine-tuned, and submitted to comparative analysis. The S2 method, as was previously shown by Gamage and Lasenby (2002), had the overall worst performance and was highly sensitive to the range of movement. Its use is, therefore, strongly discouraged. The MD and FA methods were improved relative to previous implementations. The former method reached a sustainable computational cost without affecting accuracy, and the latter method achieved better accuracy and precision. The improved MD and FA methods and the S4 method exhibited similar performances in terms of both accuracy and precision. However, the bias in the S4 method was on the average lower which demonstrates the effectiveness of the compensation procedure proposed by Halvorsen (2003). These methods were negatively and virtually equally affected by a reduction in the hip movement amplitude.

The other inaccuracy factors submitted to analysis affected the quality of the estimate to different extents. Cluster design parameters may be critical for the performance of the MD and FA methods. The maximal expected error increased when increasing the distance of the femoral marker cluster from the CR and when reducing the cluster dimension. The latter factor amplifies the propagation of the stereophotogrammetric error to position and orientation of the rigid cluster (Cappozzo et al., 1997). The S4 method was less sensitive to both cluster parameters. In any case, markers should be placed as far as possible from each other and as close as possible to the HJC. These requirements may conflict with the necessity of locating the markers on the thigh where soft tissue artefacts may be minimal, that is, on its distal part.

A further note regards the fact that, as opposed to the MD and FA methods, the S4 method entails no geometric constraints between markers. This suggests that the S4 method may be less sensitive to the marker cluster deformation associated with soft tissue artefacts, while all methods are expected to be equally affected by the other component of this artefact, that is the rigid movement of the cluster relative to the underlying bone. In addition, the S4 method shares with the MD method the lowest computation time.

Results relative to the number of data samples suggest that it should be greater than 500. In previous investigations 240 samples were used in simulation (Halvorsen, 2002, 2003), consistent with a Cross movement (execution time ≈ 4 s) acquired at a rate of 60 samples per second. By increasing the sample number to 500 (through a higher acquisition rate or a slower task execution), δ_a is reduced by 40%. The StarArc and Arc movements yield a 40% better performance than the Cross movement when the same number of samples is acquired, irrespective of the analytical method used. This is plausibly due to a complete exploration of all degrees of freedom of the hip joint and, thus, to the gathering of more relevant information. The duration of the StarArc movement, executed at a spontaneous speed, is about 7 s, while that of the Arc movement requires approximately 3 s. Thus, the StarArc movement may be preferred in order to match the above-mentioned requirement on data number.

In summary, according to the results of this study, the following guidelines are proposed:

1. S4 algorithm;
2. StarArc movement performed at a self-selected speed;
3. range of movement as wide as possible and, in case, not lower than $15°$ in neutral to flexed, neutral to extended, neutral to adducted position (div = 2);
4. sample number greater than 500;
5. marker centroid located as close as possible to the hip joint;
6. markers located at the possible largest distance from each other.

The presence of soft tissue artefacts, not incorporated in the present analysis, may pose constraints to the guidelines relative to the marker cluster design and location and to the range of movement (guidelines 3, 5, and 6) (Cappozzo et al., 1996).

The data in Table 3 are presented in order to provide possible reasons why different authors have reported remarkably different performances while using the functional method, and to assess the consistency of the results of the present investigation with those available in the literature. Most authors have used the Cross movement (Bell et al., 1990, Leardini et al., 1999, Halvorsen, 2003, Hicks et al., 2003) and have not considered marker cluster design as a critical issue. Moreover the use of a low sampling frequency (~ 60 samples per second) has often implied the collection of a low number of samples. These considerations brought to the following definition of a paradigmatic worst realistic case: Cross movement; $l = 120$ mm; $\rho = 500$ mm; $div = 2$; $N = 240$. The same was done using parameters that were consistent with the above-listed good practice guidelines. Going from the worst to the best set up, simulation results improved on average by a factor of ten (Table 3). The experimental parameters used and the results obtained by Leardini et al. (1999), Piazza et al. (2001) and Halvorsen (2002, 2003) are also reported. The data presented by Halvorsen (2002, 2003) support those obtained when complying with the guidelines. Piazza et al. (2001), using a mechanical linkage, obtained larger errors than those reported for our linkage (using the method S2). This may be explained by a noisier stereophotogrammetric system and by the smaller dimension of the marker cluster. Leardini et al. (1999) report a much larger bias that can be associated

Table 3
Results obtained in previous studies by different authors and in this study with parameters set at values that would mimic the worst realistic case or consistent with the guidelines

		Trials	e_s (mm)	l (mm)	ρ (mm)	N	Movement	Div	S2		S4		MD		FA	
									σ_a (mm)	b_a (mm)	σ_a (mm)	b_a (mm)	σ_a (mm)	b_a (mm)	σ_a (mm)	b_a (mm)
Leardini et al. (1999)	In vivo	—	≈1	≈120	≈400	—	*Cross*	1.5	4.1	11.8	—	—	—	—	—	—
Halvorsen (2002)	Simulation	100	1	200	200	240	*Cross*	1.5	—	—	0.5	0.05	0.3	0.3	0.3	0.3
Halvorsen (2003)	Simulation	100	1	200	200	240	*Cross*	1.5	—	—	0.5	0.03	—	—	—	—
Piazza et al. (2001)	Mechanical hinge	—	—	≈60	200	—	*Cross*	1	1.8	4.4	—	—	—	—	—	—
								2	16.4	7.8	—	—	—	—	—	—
							Arc	1	1.8	4.4	—	—	—	—	—	—
								2	10.5	7.6	—	—	—	—	—	—
Worst realistic case	Simulation	50	1	120	500	240	*Cross*	2	5.5	0.7	2.8	0.7	2.6	1.9	2.5	4.9
	Mechanical hinge	10	0.3	120	500	≈240	*Cross*	2	1.5	2.8	0.9	2.5	0.7	4.2	0.9	4.8
According to the guidelines	Simulation	50	1	200	300	500	*StarArc*	1	0.6	0.1	0.3	0.07	0.2	0.05	0.2	0.07
	Mechanical hinge	10	0.3	200	300	>1000	*StarArc*	1	0.9	<1	0.5	<1	0.9	<1	0.9	<1

with the fact that their results were obtained in vivo and were affected by soft tissue artefacts.

After the above-mentioned guidelines have been completed by incorporating the issues related with soft tissue artefacts and pelvic anatomical landmark identification errors, and have been agreed upon, a multi-centre endeavour may be proposed aimed at gathering a large amount of data using the functional method, under selected experimental conditions and with selected population samples. The database thus obtained could then be used to determine population-specific predictive models.

Acknowledgements

References

Aguinaldo, A.L., Wyatt, M.P., Chambers, H.G., Sutherland, D.H., 2003. Accuracy of a functional method of locating the joint center of the abnormal hip: a validation study using MRI. In: Proceedings of the Eighth Gait and Clinical Movement Analysis Meeting. University of Delaware, Wilmington, Delaware, USA.

Alderink, G., Cobabe, Y., Foster, R., Marchinda, D., 2000. Intra- and inter-rater reliability of specific pelvic and leg measurements used for determining hip joint center. In: Proceedings of the Fifth Gait and Clinical Movement Analysis Meeting. Mayo Clinic, Rochester, Minnesota, USA.

Andriacchi, T.P., Andersson, G.B., Fermier, R.W., Stern, D., Galante, J.O., 1980. A study of lower-limb mechanics during stair-climbing. Journal of Bone and Joint Surgery 62, 749–757.

Bell, A.L., Brand, R.A., Pedersen, D.R., 1989. Prediction of Hip-Joint Center Location from External Landmarks. Human Movement Science 8, 3–16.

Bell, A.L., Pedersen, D.R., Brand, R.A., 1990. A comparison of the accuracy of several hip joint center location prediction methods. Journal of Biomechanics 23, 617–621.

Besier, T.F., Sturnieks, D.L., Alderson, J.A., Lloyd, D.G., 2003. Repeatability of gait data using a functional hip joint centre and a mean helical knee axis. Journal of Biomechanics 36, 1159–1168.

Cappozzo, A., 1984. Gait analysis methodology. Human Movement Science 3, 27–50.

Cappozzo, A., 1991. Three-dimensional analysis of human walking: experimental methods and associated artefacts. Human Movement Science 10, 589–602.

Cappozzo, A., Catani, F., Della Croce, U., Leardini, A., 1995. Position and orientation in space of bones during movement: anatomical frame definition and determination. Clinical Biomechanics 10, 171–178.

Cappozzo, A., Catani, F., Leardini, A., Benedetti, M.G., Della Croce, U., 1996. Position and orientation in space of bones during movement: experimental artefacts. Clinical Biomechanics 11, 90–100.

Cappozzo, A., Cappello, A., Della Croce, U., Pensalfini, F., 1997. Surface-marker marker cluster design criteria for 3-D bone movement reconstruction. IEEE Transactions on Biomedical Engineering 44, 1165–1174.

Cereatti, A., Camomilla, V., Cappozzo, A., 2004. Estimation of the centre of rotation: a methodological contribution. Journal of Biomechanics 37, 413–416.

Crowninshield, R.D., Johnston, R.C., Andrews, J.G., Brand, R.A., 1978. A biomechanical investigation of the human hip. Journal of Biomechanics 11, 75–85.

Davis, R.B., Ounpuu, S., Tyburski, D., Gage, R., 1991. A gait analysis data collection and reduction technique. Human Movement Science 10, 575–587.

Della Croce, U., Cappozzo, A., 2000. A spot check for estimating stereophotogrammetric errors. Medical & Biological Engineering and Computing 38, 260–266.

Fieser, L., Quigley, E., Wyatt, M., Sutherland, D., Chambers, H., 2000. Comparison of hip joint centers determined from surface anatomy and CT scans: two case studies. In: Proceedings of the Fifth Gait and Clinical Movement Analysis Meeting. Mayo Clinic, Rochester, Minnesota, USA.

Gamage, S.S.H.U., Lasenby, J., 2002. New least squares solutions for estimating the average centre of rotation and the axis of rotation. Journal of Biomechanics 35, 87–93.

Halvorsen, K., 2002. Model-based methods in motion capture. Ph.D. Thesis, Acta Universitatis Upsaliensis, Uppsala Dissertations from the Faculty of Science and Technology, 42, ISBN:91-554-5381-3.

Halvorsen, K., 2003. Bias compensated least square estimate of the center of rotation. Journal of Biomechanics 36, 999–1008.

Halvorsen, K., Lesser, M., Lundberg, A., 1999. A new method for estimating the axis of rotation and the center of rotation. Journal of Biomechanics 32, 1221–1227.

Hicks, J., Richards, J., Hudson, D., Henley, J., 2003. Clinical implications of using spherical fitting to find hip joint centers. In: Proceedings of the Eighth Gait and Clinical Movement Analysis Meeting. University of Delaware, Wilmington, Delaware, USA.

Holden, J.P., Stanhope, S.J., 1998. The effect of variation in knee center location estimate on net knee joint moments. Gait Posture 7, 1–6.

Holzreiter, S., 1991. Calculation of the instantaneous centre of rotation for a rigid body. Journal of Biomechanics 24, 643–647.

Jenkins, S.M.E., Harrington, M.E., Elliot, M., Theologis, T.N., O'Connor, J.J., 2000. The customisation of a three dimensional locomotor model to children. In: Proceedings of the Sixth International Symposium on 3-D Analysis of Human Movement. Cape Town, South Africa.

Kapandji, I.A., 1987. The Physiology of Joints. Lower Limb. Vol. 2. Churchill Livingstone, London, pp. 2–15.

Kirkwood, R.N., Culham, E.G., Costigan, P., 1999. Radiographic and non-invasive determination of the hip joint center location: effect on hip joint moments. Clinical Biomechanics 14, 227–235.

Lagarias, J.C., Reeds, J.A., Wright, M.H., Wright, P.E., 1998. Convergence properties of the Nelder-Mead simplex method in low dimensions. SIAM Journal of Optimization 9, 112–147.

Leardini, A., Cappozzo, A., Catani, F., Toksvig-Larsen, S., Petitto, A., Sforza, V., Cassanelli, G., Giannini, S., 1999. Validation of a functional method for the estimation of hip joint centre location. Journal of Biomechanics 32, 99–103.

Lenhoff, M.W., Shea, K.M., Otis, J.C., Backus, S.I., 1998. Location of the hip joint center in gait analysis. Gait and Posture 7, 179–180.

Neptune, R.R., Hull, M.L., 1995. Accuracy assessment of methods for determining hip movement in seated cycling. Journal of Biomechanics 28, 423–437.

Piazza, S.J., Okita, N., Cavanagh, P.R., 2001. Accuracy of the functional method of hip joint centre location: effects of limited motion and varied implementation. Journal of Biomechanics 34, 967–973.

Piazza, S.J., Erdemir, A., Okita, N., Cavanagh, P.R., 2004. Assessment of the functional method of hip joint center location to reduced range of hip motion. Journal of Biomechanics 37, 349–356.

Schwartz, M., Rozumalski, A., 2003. The reliability of two dynamic methods for hip joint center estimation. In: Proceedings of the Eighth Gait and Clinical Movement Analysis Meeting. University of Delaware, Wilmington, Delaware, USA.

Seidel, G.K., Marchinda, D.M., Dijkers, M., Soutas-Little, R.W., 1995. Hip joint center location from palpable bony landmarks—a cadaver study. Journal of Biomechanics 28, 995–998.

Silaghi, M., Plaenkers, R., Boulic, R., Fua, P., Thalmann, D., 1998. Local and global skeleton fitting techniques for optical motion capture. In: Magnenat-Thalmann, N., Thalmann, D. (Eds.), Modelling and Motion Capture Techniques for Virtual Environments, Lecture Notes in Artificial Intelligence. Springer, Berlin, pp. 26–40 No. 1537.

Söderkvist, I., Wedin, P.A., 1993. Determining the movements of the skeleton using well-configured markers. Journal of Biomechanics 26, 1473–1477.

Stagni, R., Leardini, A., Cappozzo, A., Benedetti, M.G., Cappello, A., 2000. Effects of hip joint centre mislocation on gait analysis results. Journal of Biomechanics 33, 1479–1487.

Tylkowski, C.M., Simon, S.R., Mansour, J.M., 1982. Gait in spastic cerebral palsy. The Hip: Proceedings of the Tenth Open Meeting of the Hip Society. Vol. 10, pp. 89–125.

Woltring, H.J., 1990. Data processing and error estimation. In: Berme, N., Cappozzo, A. (Eds.), Biomechanics of Human Movement: Applications in Rehabilitation, Sports and Ergonomics. Bertec, pp. 203–237.

Woltring, H.J., Huiskes, R., De Lange, A., Veldpaus, F.E., 1985. Finite centroid and helical axis estimation from noisy landmark measurements in the study of human joint kinematics. Journal of Biomechanical Engineering 18, 379–389.

Wu, G., Siegler, S., Allard, P., Kirtley, C., Leardini, A., Rosenbaum, D., Whittle, M., D'Lima, D.D., Cristofolini, L., Witte, H., Schmid, O., Stokes, I., 2002. ISB recommendation on definitions of joint coordinate system of various joints for the reporting of human joint motion–part I: ankle, hip, and spine. Journal of Biomechanics 35, 543–548.